

F-x statics for P-S seismic data

Wai-kin Chan and Robert R. Stewart

ABSTRACT

A technique of solving statics without velocity information in the f-x domain was proposed by Chan and Stewart (1996) and was tested on a structural Marmousi dataset with promising results. The major difference of this technique from conventional routines is that the correlation model is built from the f-x prediction rather than a velocity dependent stack trace. In this paper, the results of applying the f-x statics routine to the Blackfoot P-S dataset is presented. This technique is believed to be especially important in solving statics for the structural converted wave data, without depending on the asymptotic common conversion point binning.

INTRODUCTION

Most surface-consistent residual statics algorithms rely on maximizing the power of a CMP stack. However, errors in the estimated statics are strongly correlated to the NMO velocity error. As Ronen and Claerbout (1988) said, "statics estimation is effectively a velocity analysis of the near-surface. Ideally, statics and velocity analysis would be done together ". In practice, the velocity and the statics are solved iteratively. This iterative procedure works well provided that the first velocity estimation is reasonable.

In a complex structural region, reasonable velocity estimation in the presence of large statics is not possible. In general, the assumption of hyperbolic moveout in the CMP domain is violated and hence, the maximum stack power may not reflect the proper statics. The problem is even worse for converted-wave data where S-wave receiver statics are solved in the ACCP domain. Note that ACCP binning requires an estimate of the average V_p/V_s ratio, and that even for 1-D earth models this binning is only an approximation.

In this paper, an alternative method of solving statics proposed by Chan and Stewart (1996) is used to apply the Blackfoot converted-wave dataset. This new approach operates in the common offset domain and does not require a priori NMO velocity information or the assumption of hyperbolic moveout.

THEORY

The basic requirement of the new statics routine is that reflection events, without statics contamination, in the common offset plane are smooth. When statics are present, the image in each common offset plane exhibits trace-to-trace jitter, and that can be considered as random error superimposed on the smooth events. Using linear prediction iteratively in the f-x domain for each offset (Canales, 1984), the smoothness of the observed events is improved by virtue of the fact that the f-x prediction filter is estimated by a least-squares approach. The smoothed common offset plane, that is a common offset gather where every data trace is replaced by a trace predicted from neighboring information, is used as model. Once the models are created for all offsets, they are correlated with the original traces to find static shifts for each trace in the data. These static shifts are then decomposed into shot and receiver components in a surface-consistent manner. The statics are applied to the data, new models are predicted and subsequently new statics are estimated. Iterations continue until no significant change to statics estimate is detected.

CONVERTED-WAVE EXAMPLE

In this section, the new f-x based statics calculation is applied to a subset of a broadband 3-C 2-D seismic experiment conducted at the Blackfoot Field in July 1995. The vertical component data (4.5 Hz geophones) are first processed in the traditional way to obtain P-wave refraction statics and P-wave residual statics (Ronen-Claerbout residual statics calculation). The radial component data (4.5 Hz geophones) are then processed in a receiver-consistent manner. The data set is first datumed to 960 m with a P-wave replacement velocity of 3000 m/s at the shot and an S-wave replacement velocity of 1200 m/s at the receiver. As well, P-wave refraction statics and P-wave residual statics for both shots and receivers are applied.

To avoid cycle skipping due to large statics, we need to work in a lower frequency band. Unfortunately, the lower frequency signal is largely contaminated by the ground roll. To solve this problem, we suppressed the ground roll in the receiver domain and limited statics calculation to offsets larger than 1000 metres. A local slant stack procedure is also applied in the receiver domain to improve the signal-to-noise ratio. The dataset is then processed with gather-oriented minimum phase deconvolution for all receivers followed by gather-oriented zero-phase deconvolution for all shots. The processed results are then analyzed with the f-x statics calculation.

For comparison purposes, Figures 1, 2 and 3 display the ACCP stack without residual receiver statics, with conventional residual receiver statics, and with f-x statics, respectively. Both static routines improve the quality of the stack. In fact, the conventional statics gives an apparently crisper stack than the f-x statics, especially in the time window 2.25 s to 2.75 s. Figure 4 displays the f-x and the conventional statics. The first trace shown in the figure is the f-x statics solution, while the next nine traces represent the solution for nine subsequent iterations of conventional statics. By comparing the f-x statics and the last iteration of the conventional statics, it is observed that they both show similar short wavelength results from stations 2700 to 6000. It is also observed that, in the conventional statics, a constant negative shift is superimposed on stations 2020 to 2600, and a positive shift is superimposed on stations 2600 to 3500, creating a break in statics at station 2600. This suggests that a cycle skip is occurred in the conventional statics solution.

Some common offset planes before and after application of conventional and f-x residual receiver statics are shown in Figure 5 to Figure 10. Figures 5 and 6 are a comparison of the results at an offset of 2270 m. Since this offset only includes stations 4300 to 6000, the results are very similar. The next two figures (Figures 7 and 8) are at an offset of -1530 m and include stations 2020 to 4480. Here, the f-x based statics estimation approach produces smoother result than the conventional statics estimation. A discontinuity in reflection events occurs at station 2600 in the conventional statics result. Figures 9 and 10 display an offset panel of -2130 m with stations ranging from 2040 to 3880. The statics break at station 2600 is obvious in Figure 9 while it is clearly missing in Figure 10 which shows the same offset corrected with f-x based statics estimates.

The next comparison involves statics application in the shot record domain. Figure 11 displays a shot record at station 4180 without residual receiver statics applied. Figures 12 and 13 are the same shot record after the application of conventional and f-x statics respectively. Both statics improve the smoothness of the reflections, except for a discontinuity at station 2600 in the conventional statics result. The next three figures (Figures 14 to 16) show the same comparison for a shot at station 5120, where the same observations hold.

The final definitive observation stage is the receiver stack domain. Figure 17 displays the receiver stack without residual receiver statics application. Figure 18 shows receiver stack with the conventional statics applied. From this figure we conclude that the statics are generally properly resolved except at the vicinity of station 2600. Note that although the raw receiver stack is wavy around station 2600, no discontinuity is seen there. Figure 19 shows a receiver stack with f-x statics applied. It is observed that the coherency of events is improved, without a discontinuity at station 2600.

CONCLUSIONS

From the previous examples one can see that the reflector smoothness condition is powerful enough to allow a robust statics estimation procedure. Since this procedure operates in the common offset domain, no prior NMO velocity information is required and hence the approach is deemed suitable for the studies of converted P-S mode data. Note that although an ACCP stack is displayed in Figure 3, the associated statics are totally independent of ACCP binning. Conventional statics routine introduces a discontinuity whereas the f-x procedure gives a plausible smoother section.

REFERENCES

- Chan, W.-K., and Stewart, R. R., 1996, f-x statics: CREWES Research Report, 8, 15.1-15.13.
Canales, L. L., 1984, Random noise reduction: Presented at the 54th Ann. Internat. Mtg., Soc. Expl. Geophys., Expanded Abstracts, 525-527.
Ronen, J. and Claerbout, J., 1985, Surface-consistent residual statics estimation by stack power maximization: *Geophysics*, 50, 2759-2767.

ACKNOWLEDGEMENTS

Data Modeling Inc., Calgary is gratefully acknowledged for the guidance throughout this study.

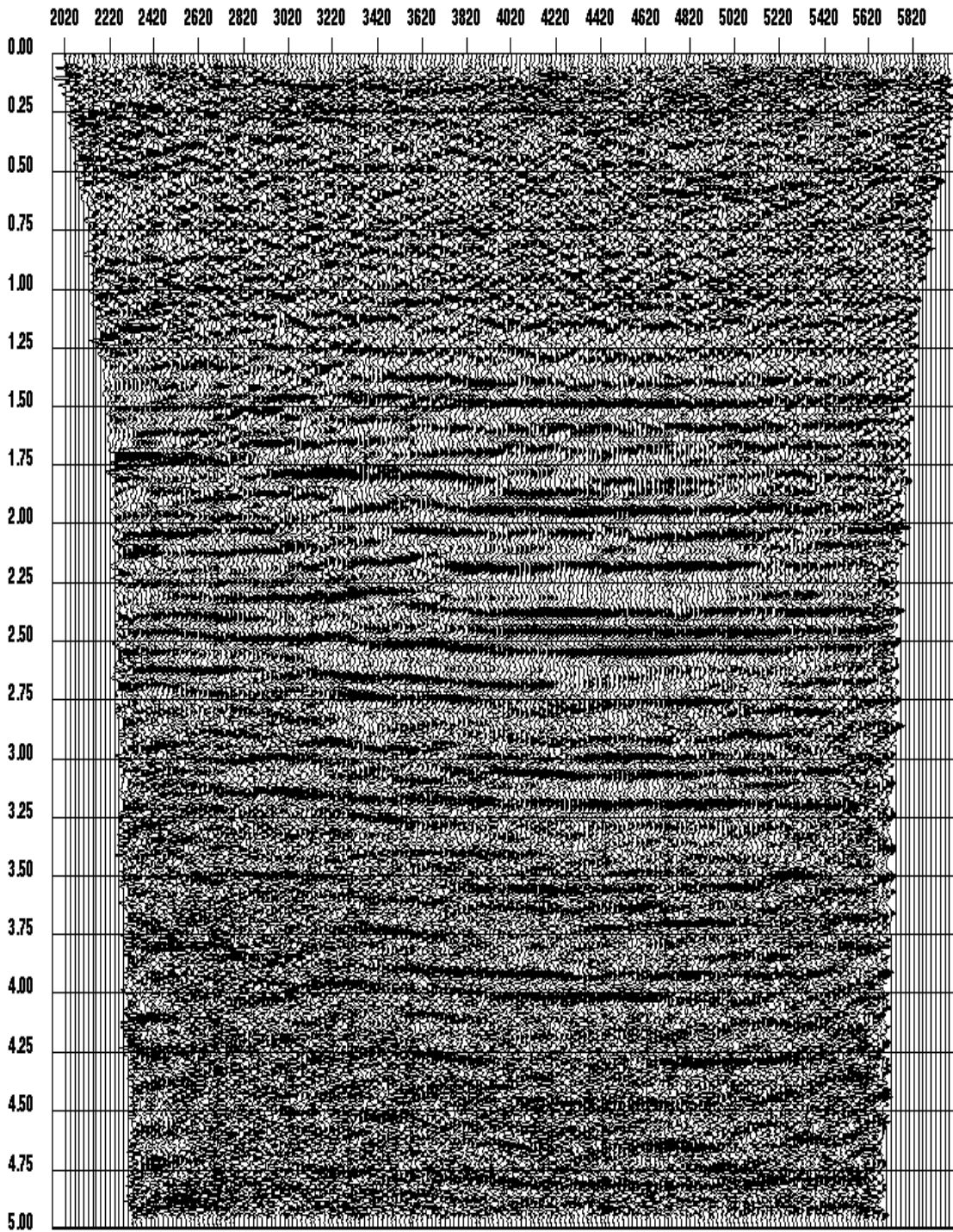


Fig. 1. ACCP stack without residual receiver statics applied.

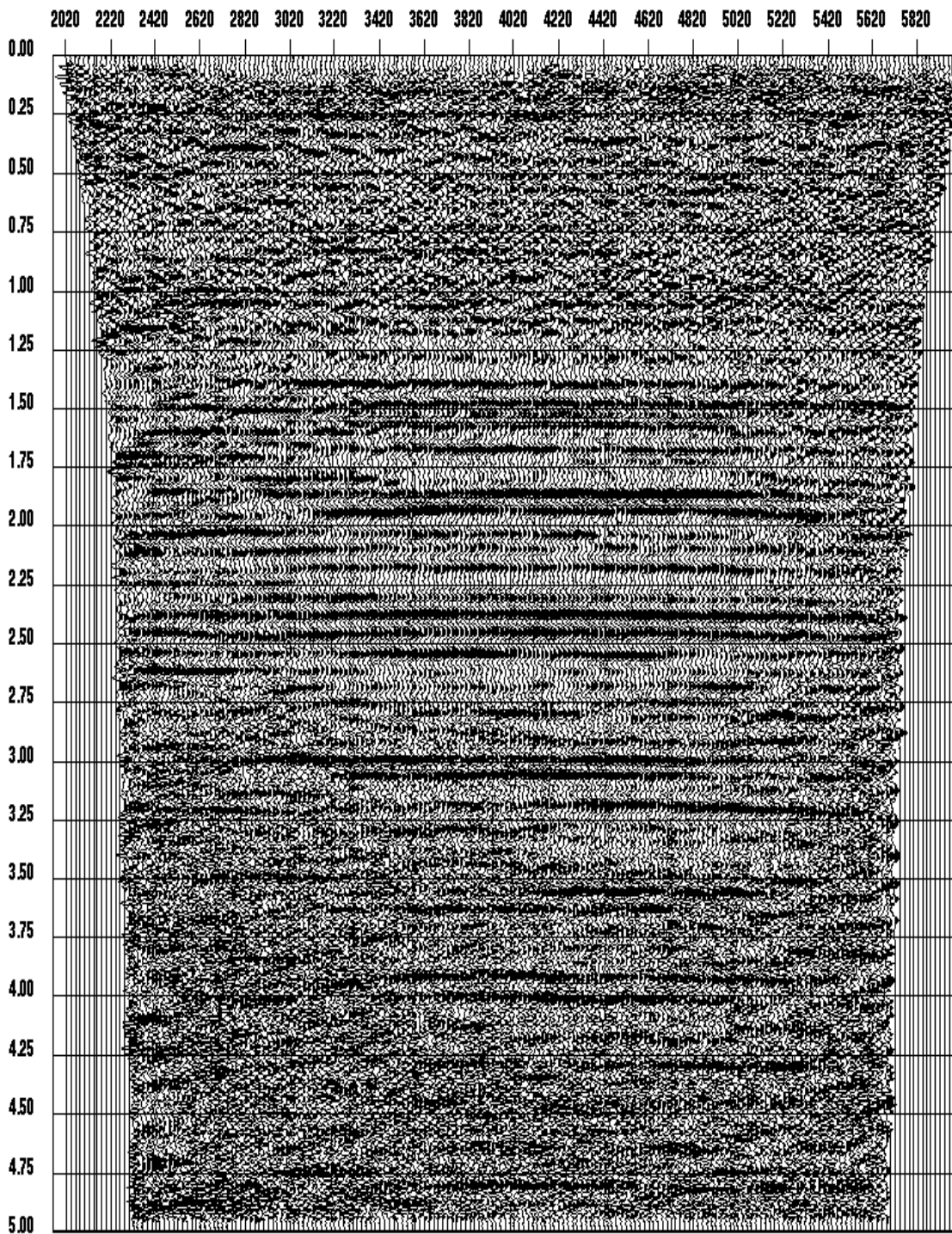


Fig. 2. ACCP stack with conventional residual receiver statics. The quality of the stack is considerably improved.

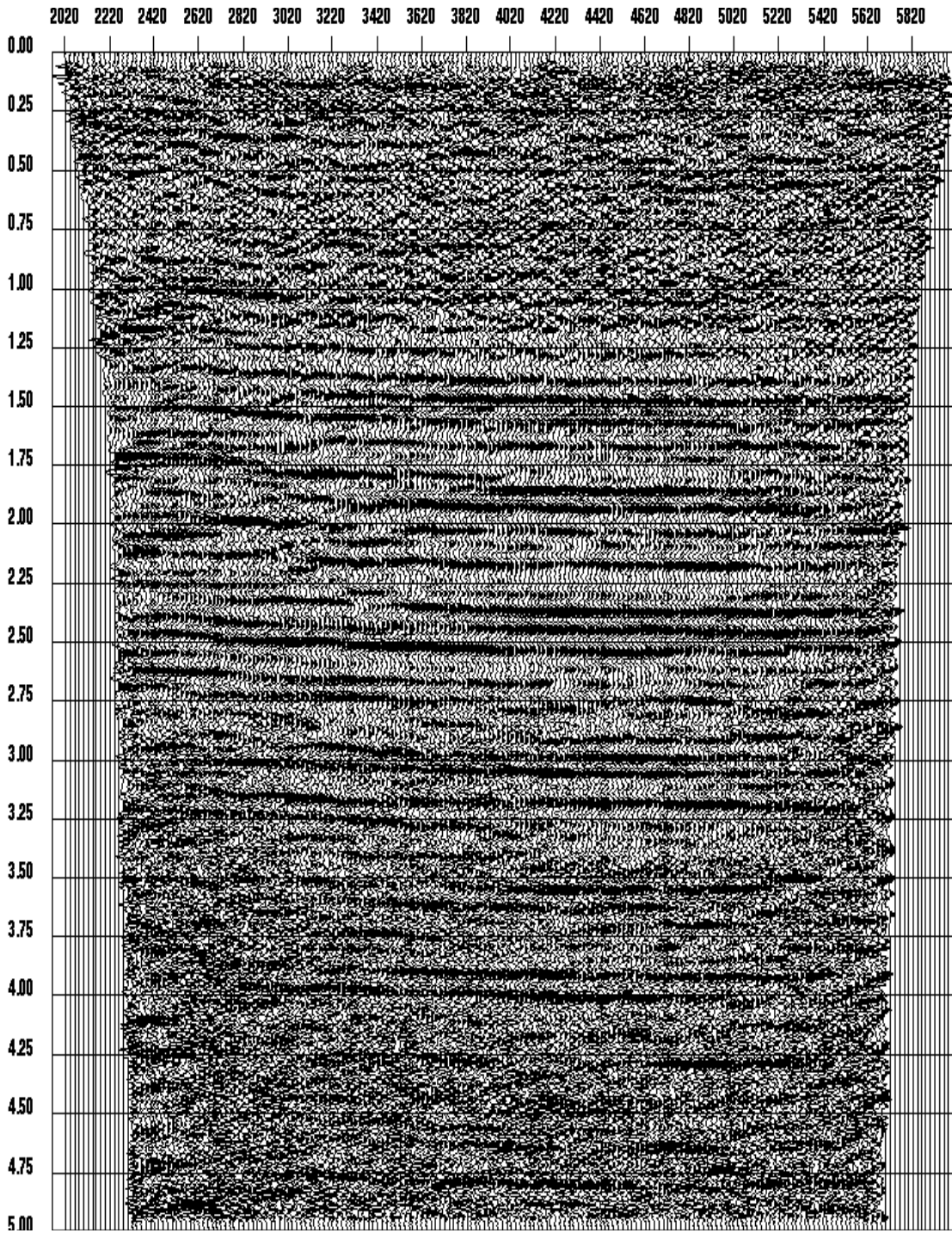


Fig. 3. ACCP stack with f-x residual statics. The quality of the stack is better than the stack without residual receiver statics, but not as high as that of the stack with conventional residual receiver statics.

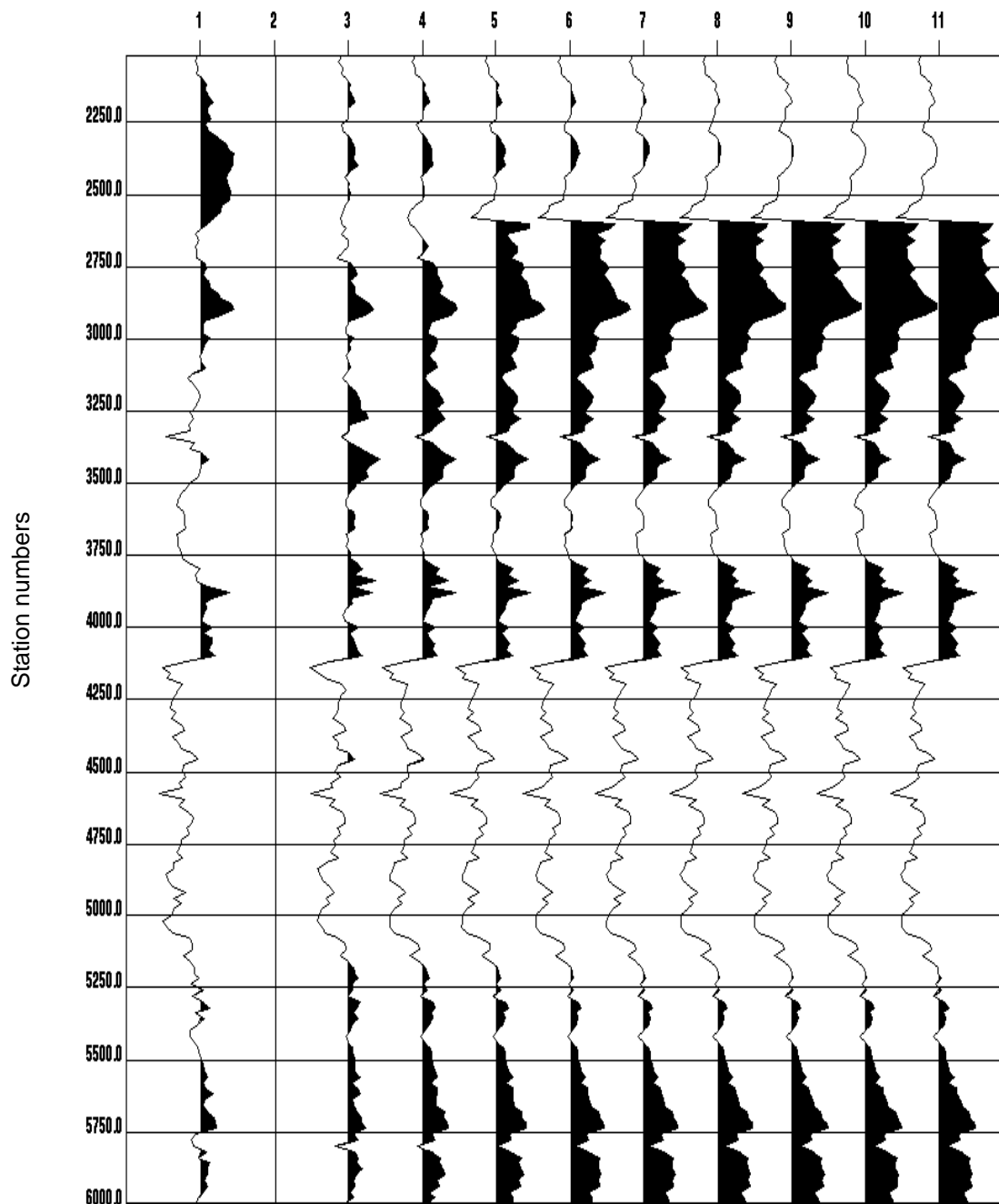


Fig. 4. Comparison of the results of f-x statics application and the Ronen and Claerbout statics. f-x statics is shown in the first trace. The first nine iterations of the Ronen and Claerbout statics are shown in the next nine traces. Both algorithms show similar results from receiver stations between 2700 to 6000. Starting from the third iteration of the Ronen and Claerbout algorithm, a D.C. bias of the statics around receiver station 2600 is built-up, and eventually it develops into a cycle-skip.

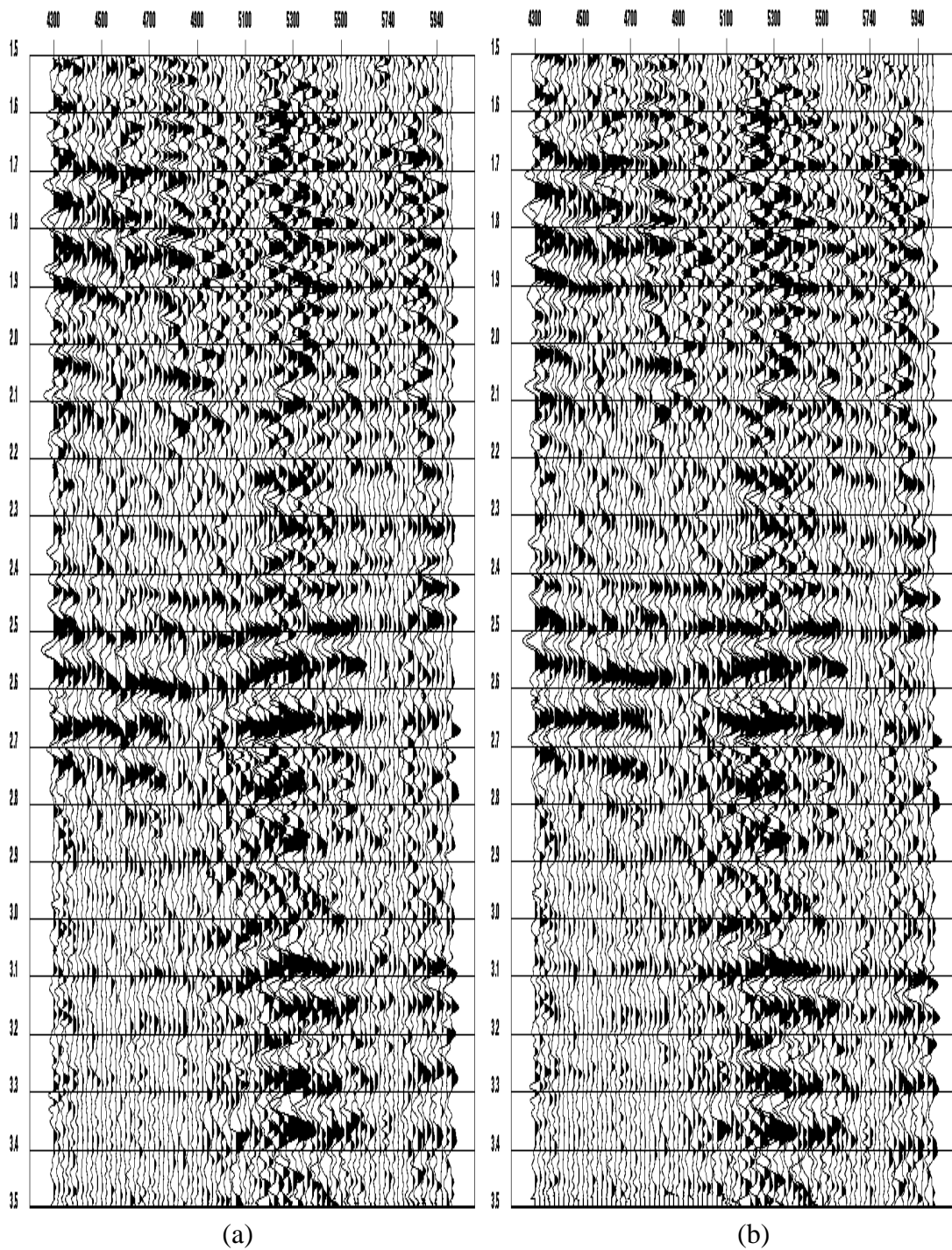


Fig. 5. A common offset plane at 2270 m. (a) Without residual receiver statics. (b) With conventional residual receiver statics.

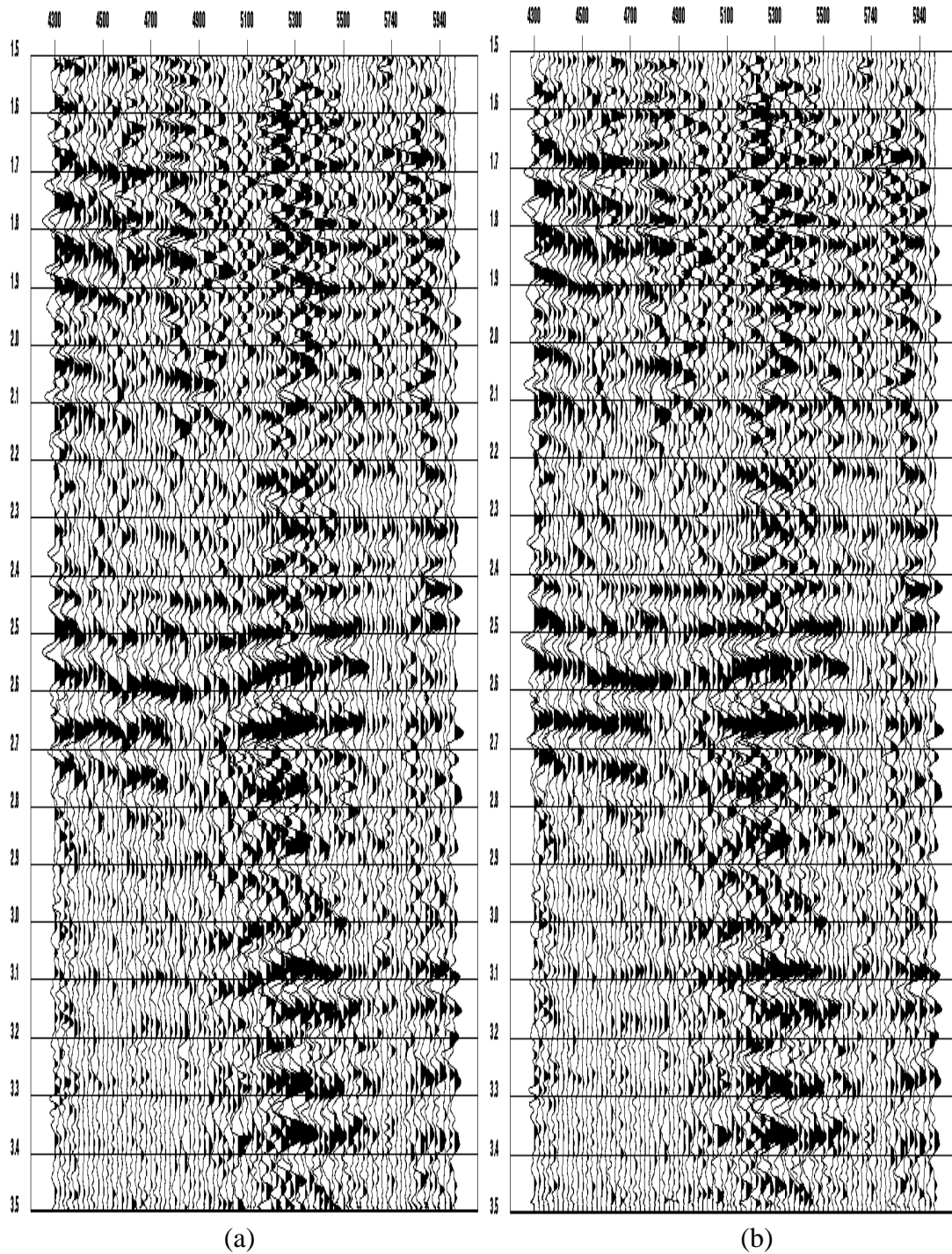


Fig. 6. A common offset plane at 2270 m. (a) Without residual receiver statics. (b) With f-x residual receiver statics.

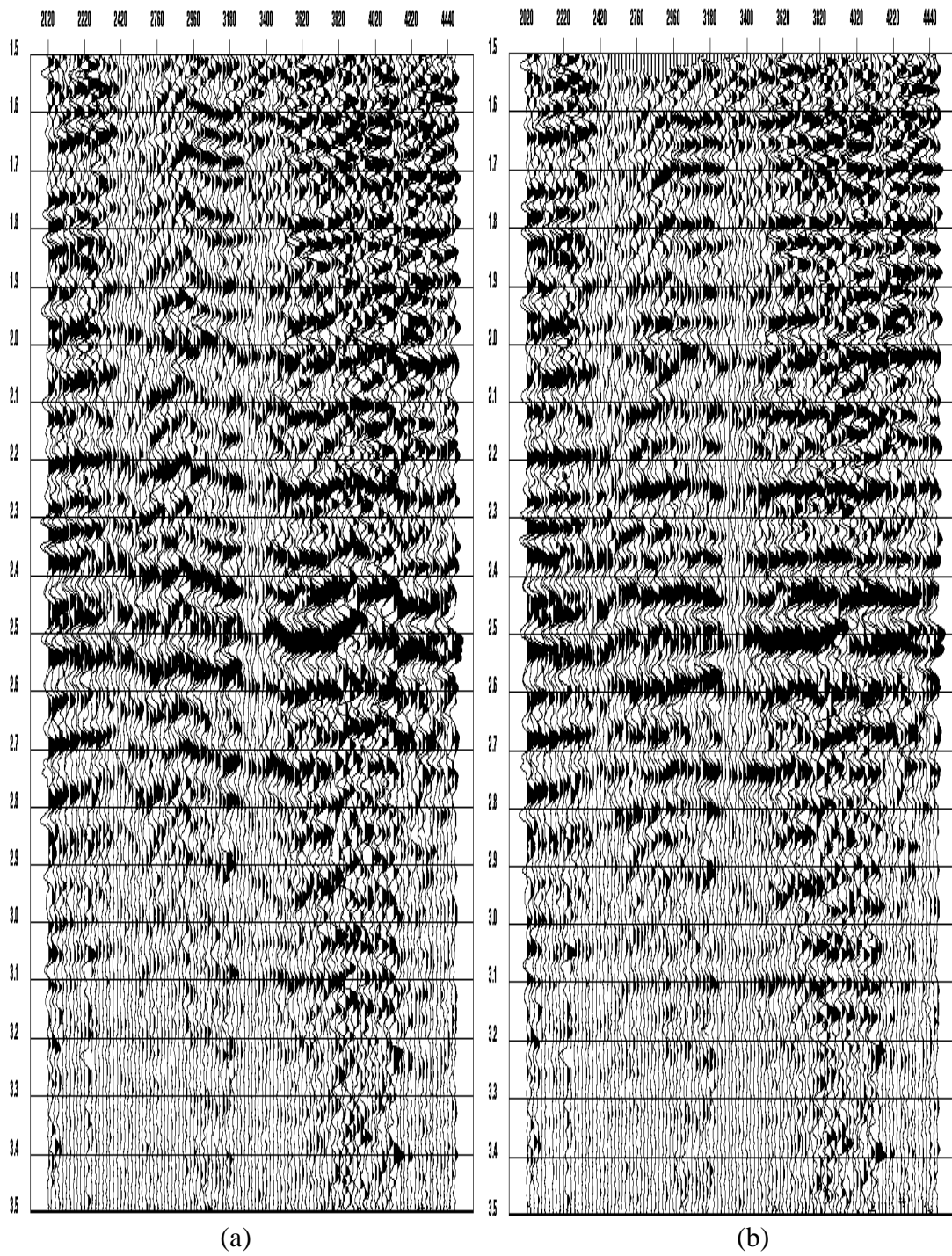


Fig. 7. A common offset plane at -1530 m. (a) Without residual receiver statics. (b) With conventional residual receiver statics.

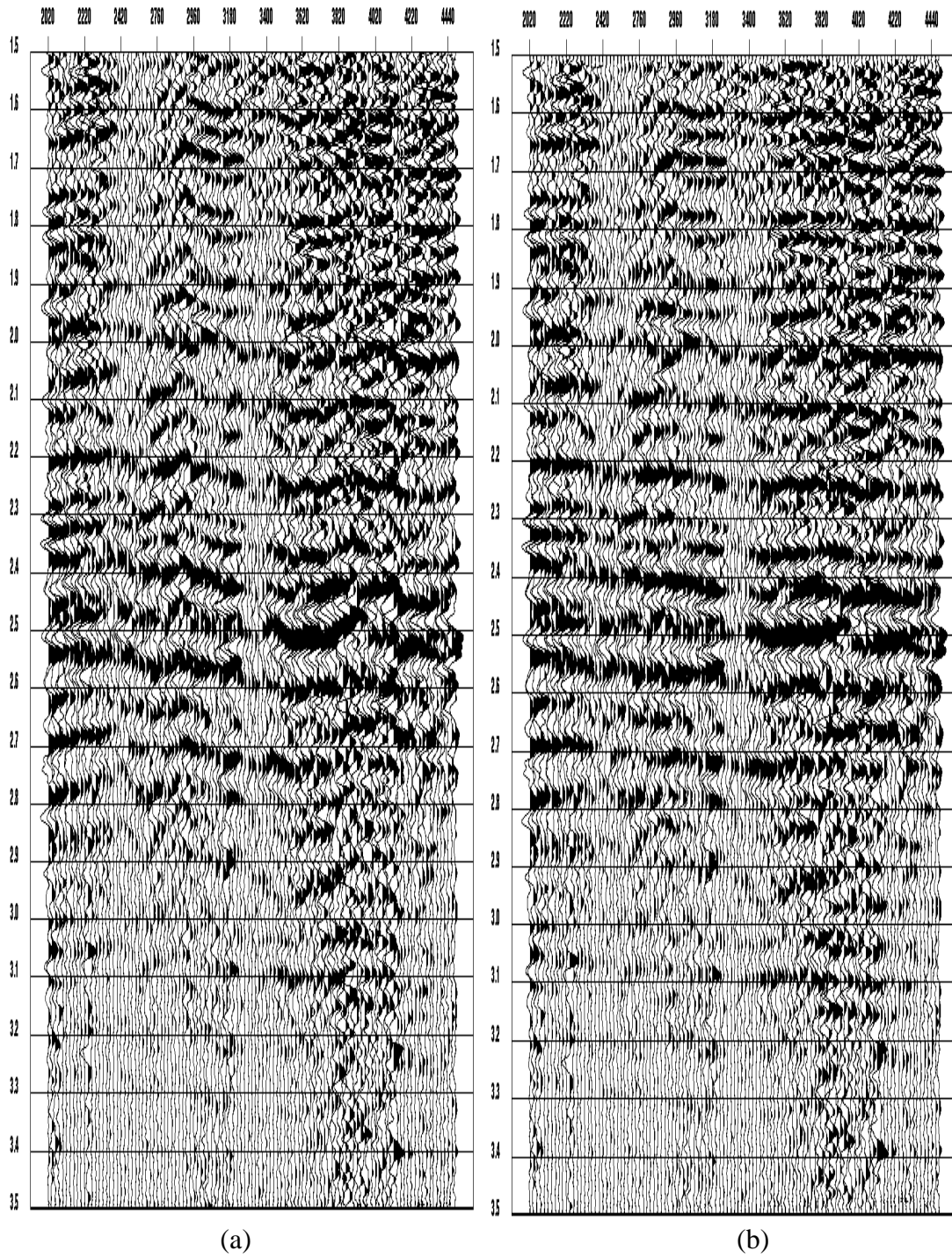


Fig. 8. A common offset plane at -1530 m. (a) Without residual receiver statics. (b) With f-x residual receiver statics.

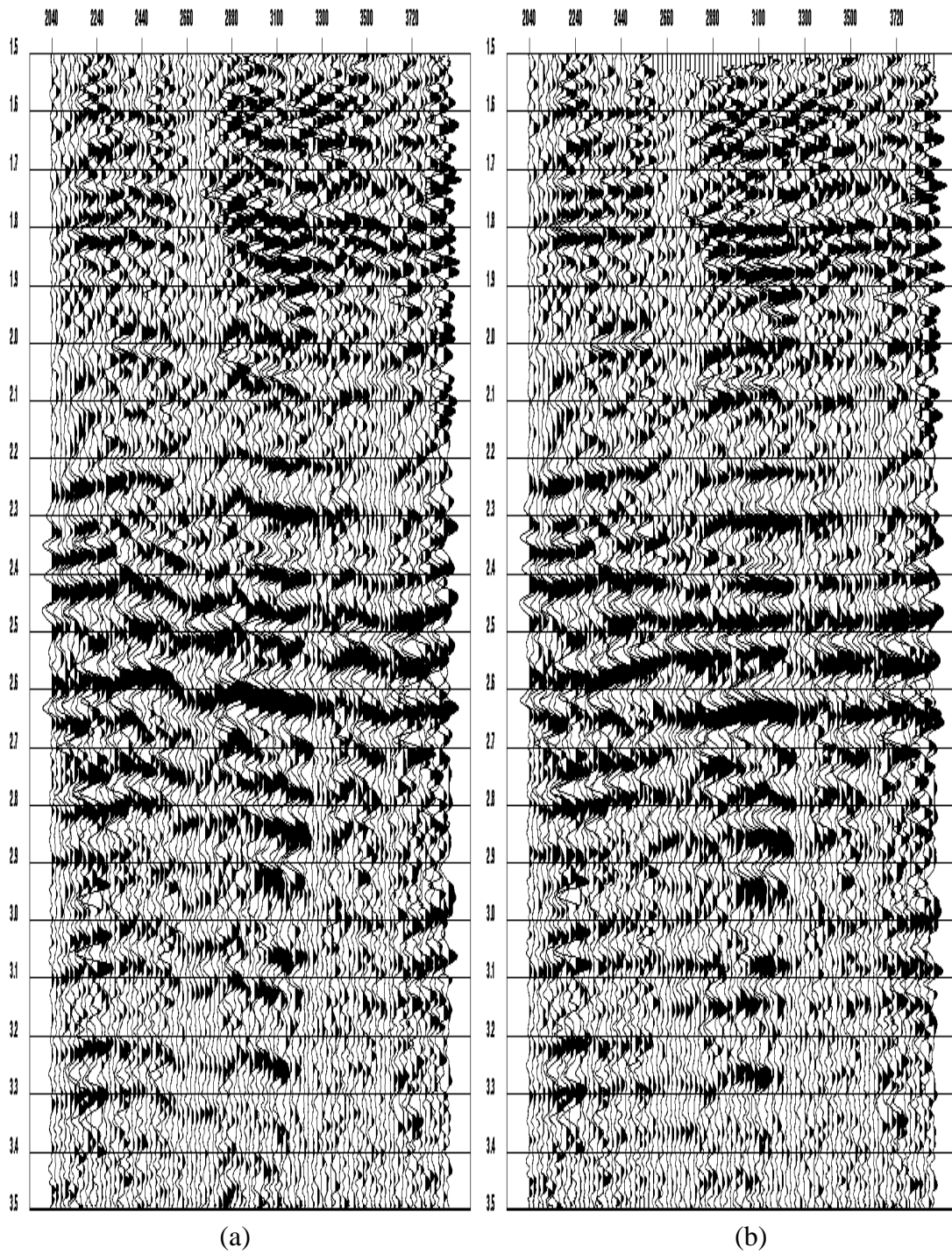


Fig. 9. A common offset plane at -2130 m. (a) Without residual receiver statics. (b) With conventional residual receiver statics.

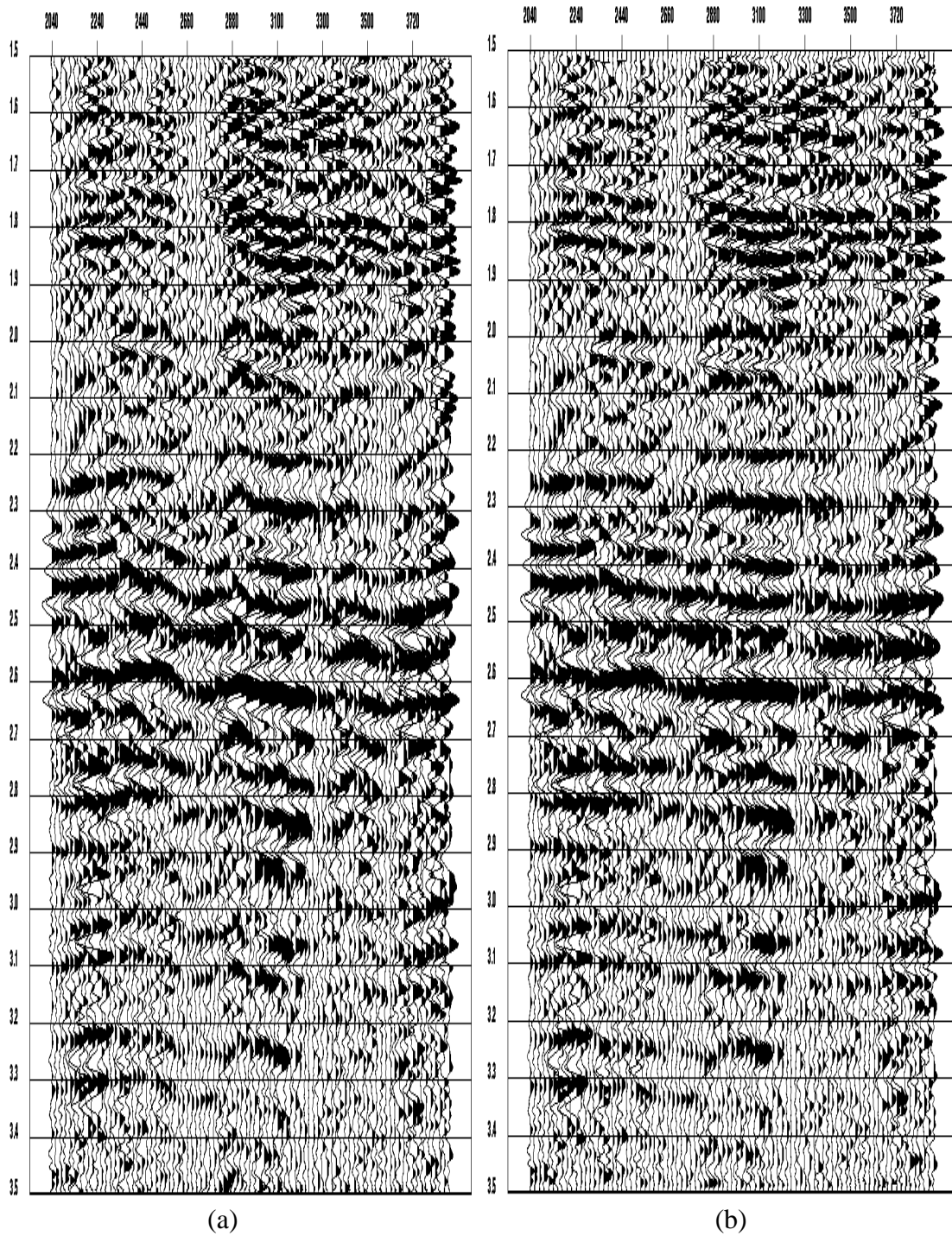


Fig. 10. A common offset plane at -2130 m. (a) Without residual receiver statics. (b) With f-x residual receiver statics.

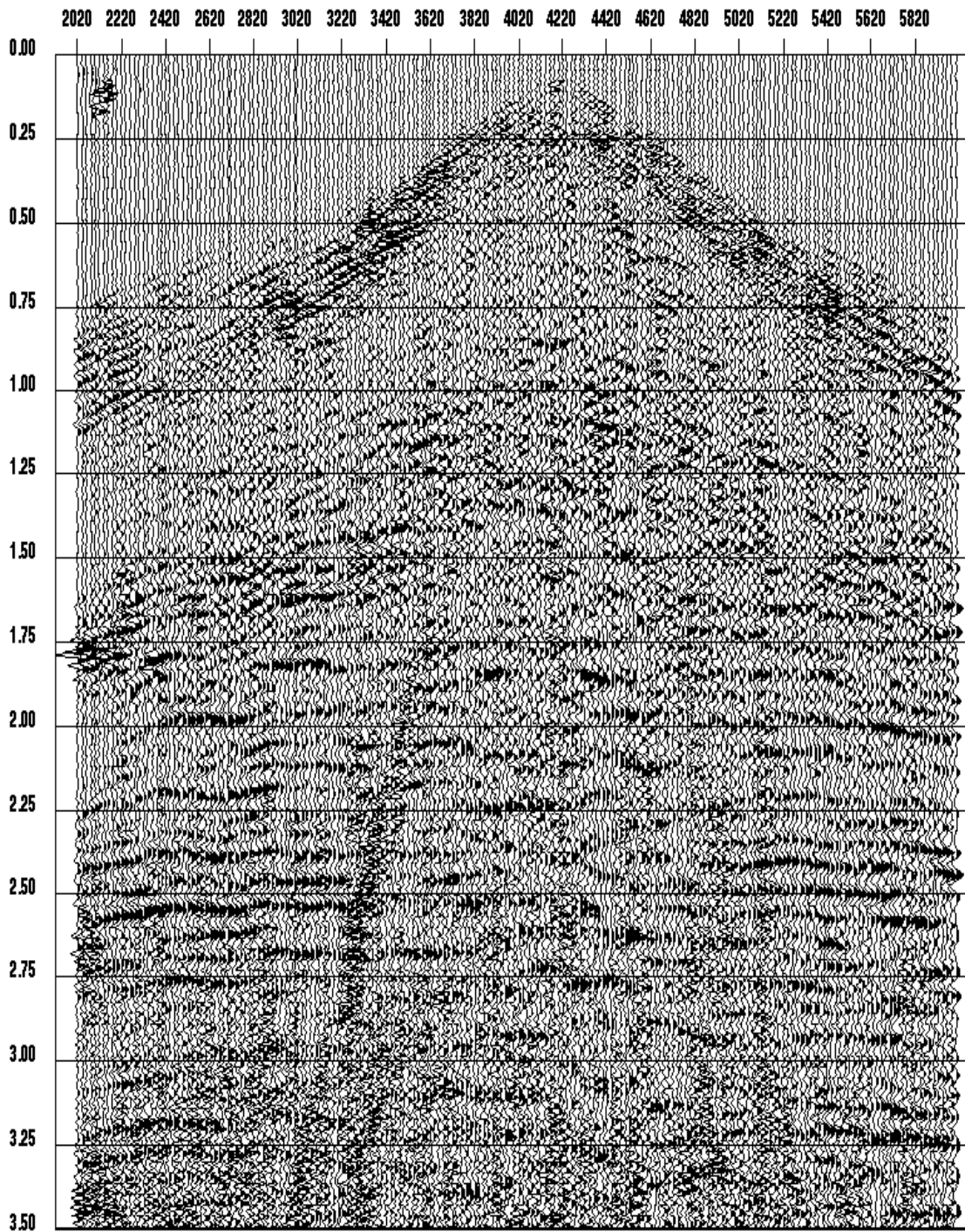


Fig. 11. Shot record at 4180 without residual receiver statics applied.

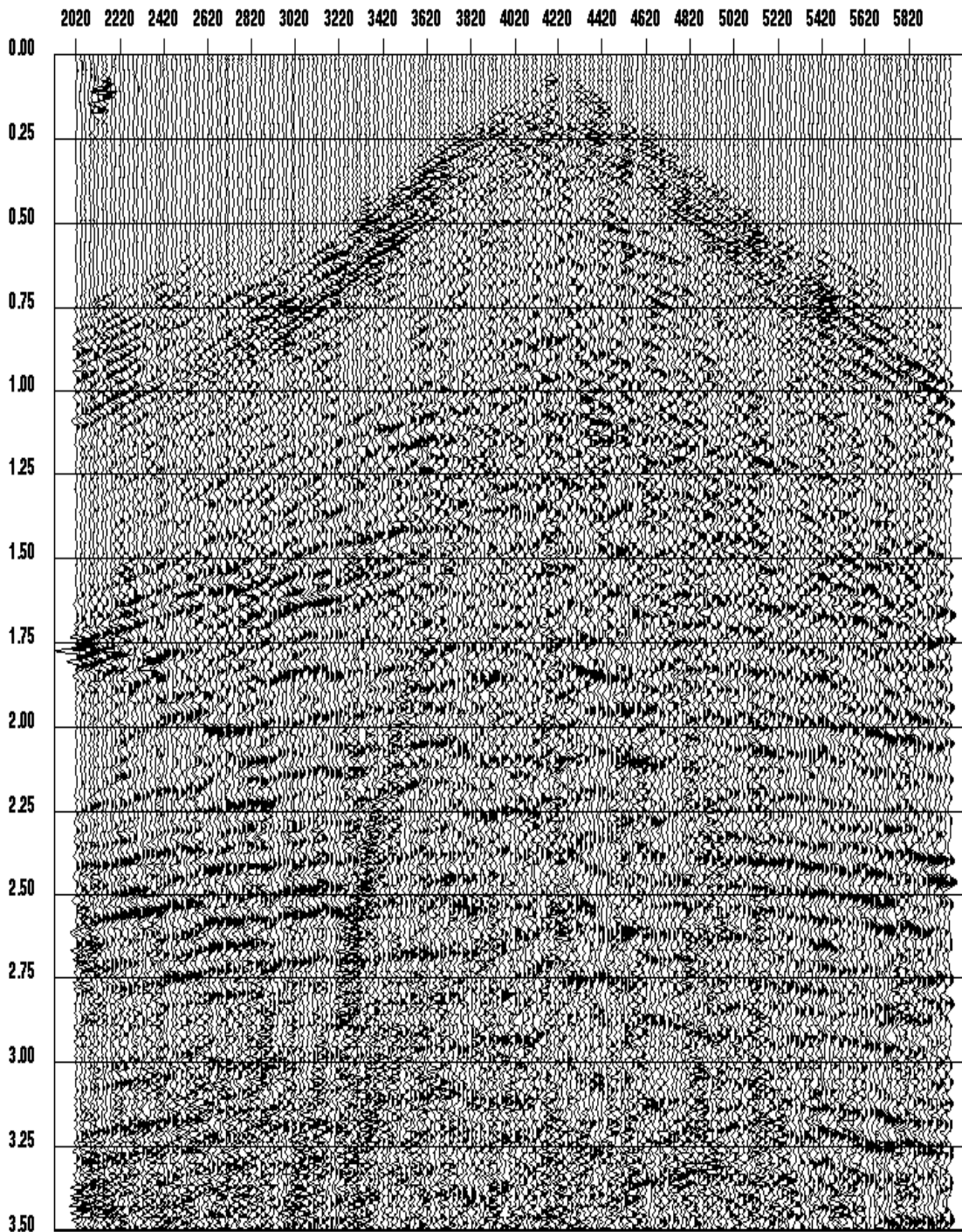


Fig. 12. Shot record at 4180 with conventional residual receiver statics applied.

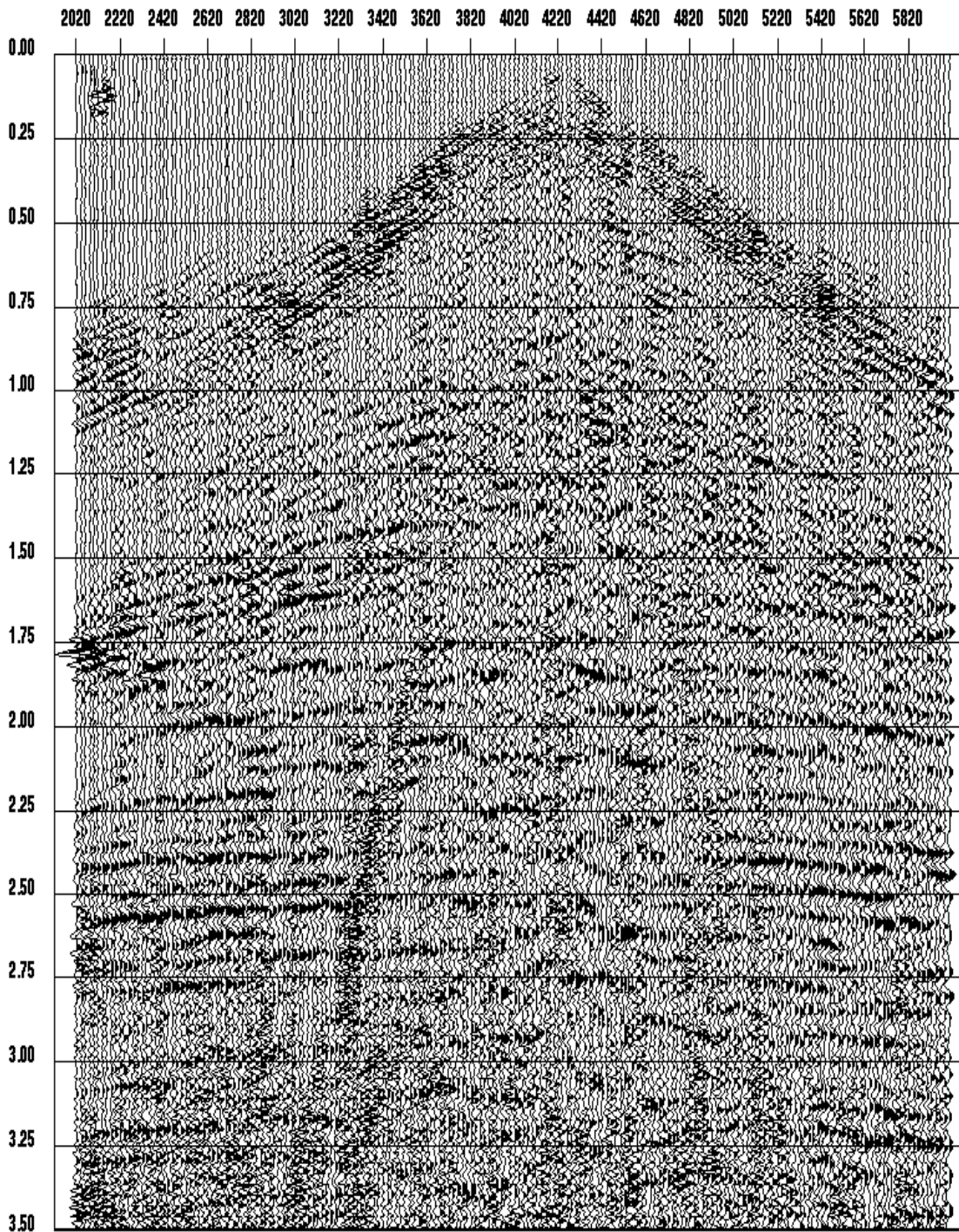


Fig. 13. Shot record at 4180 with f-x residual receiver statics applied.

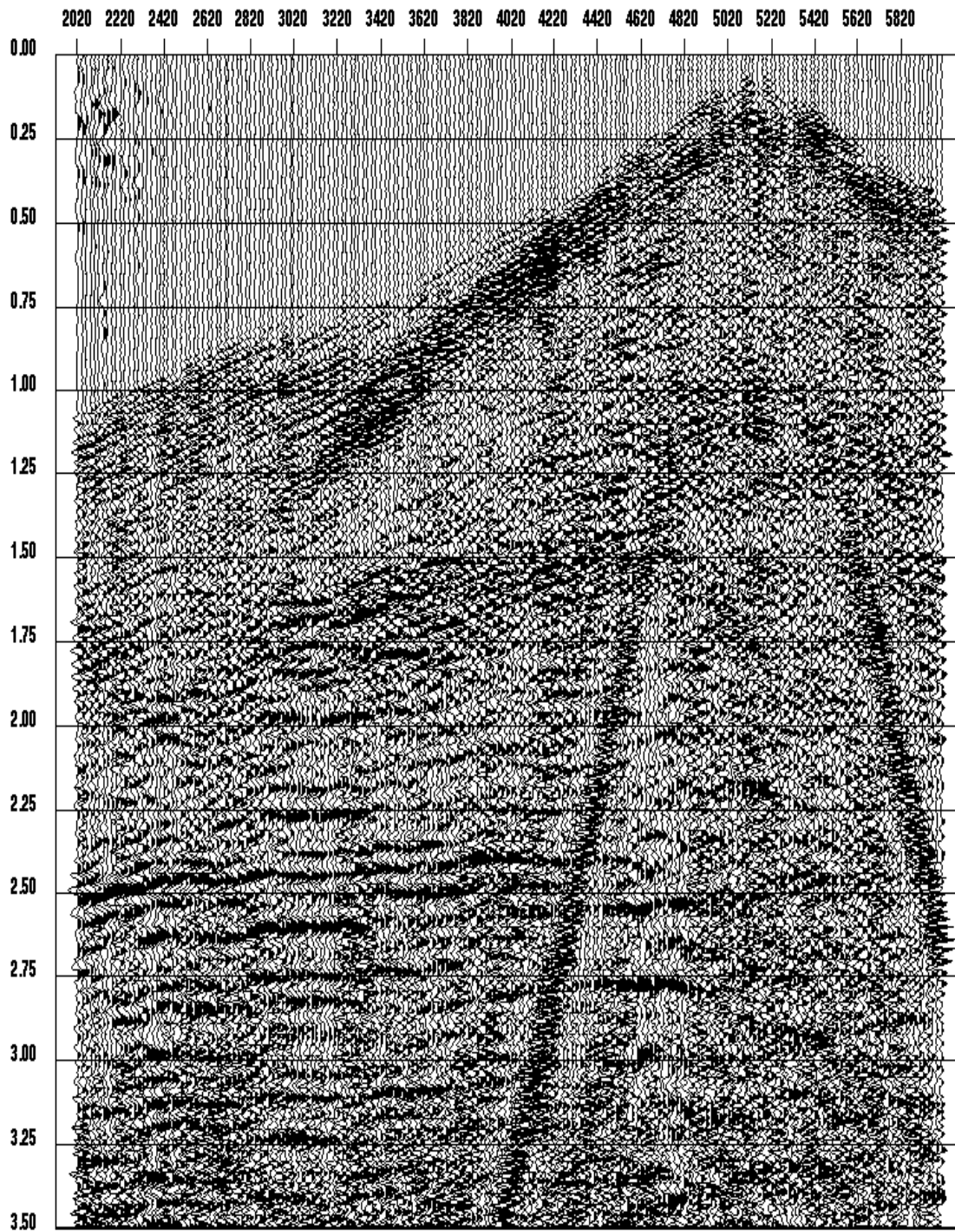


Fig. 14. Shot record at 5120 without residual receiver statics applied.

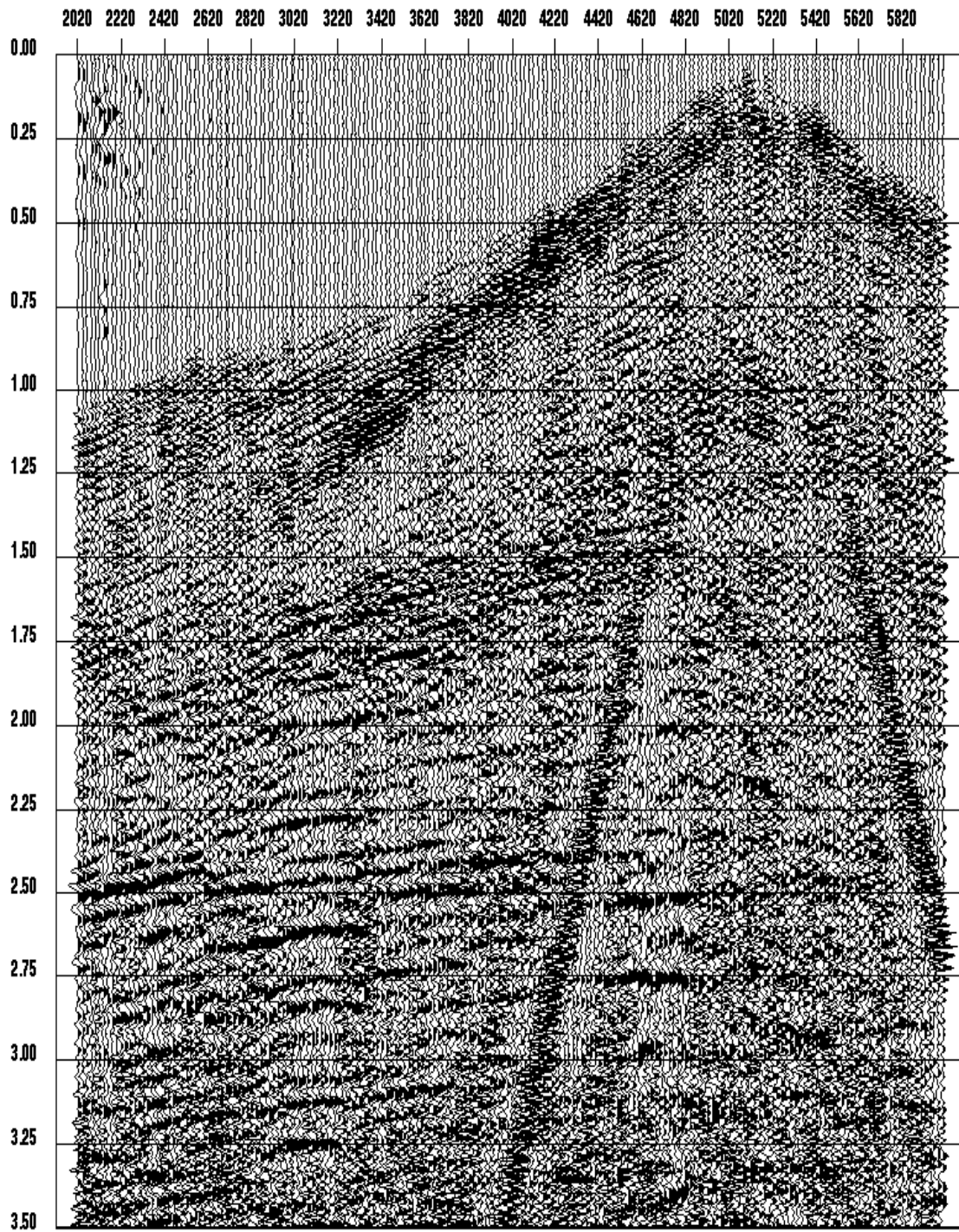


Fig. 15. Shot record at 5120 with conventional residual receiver statics applied.

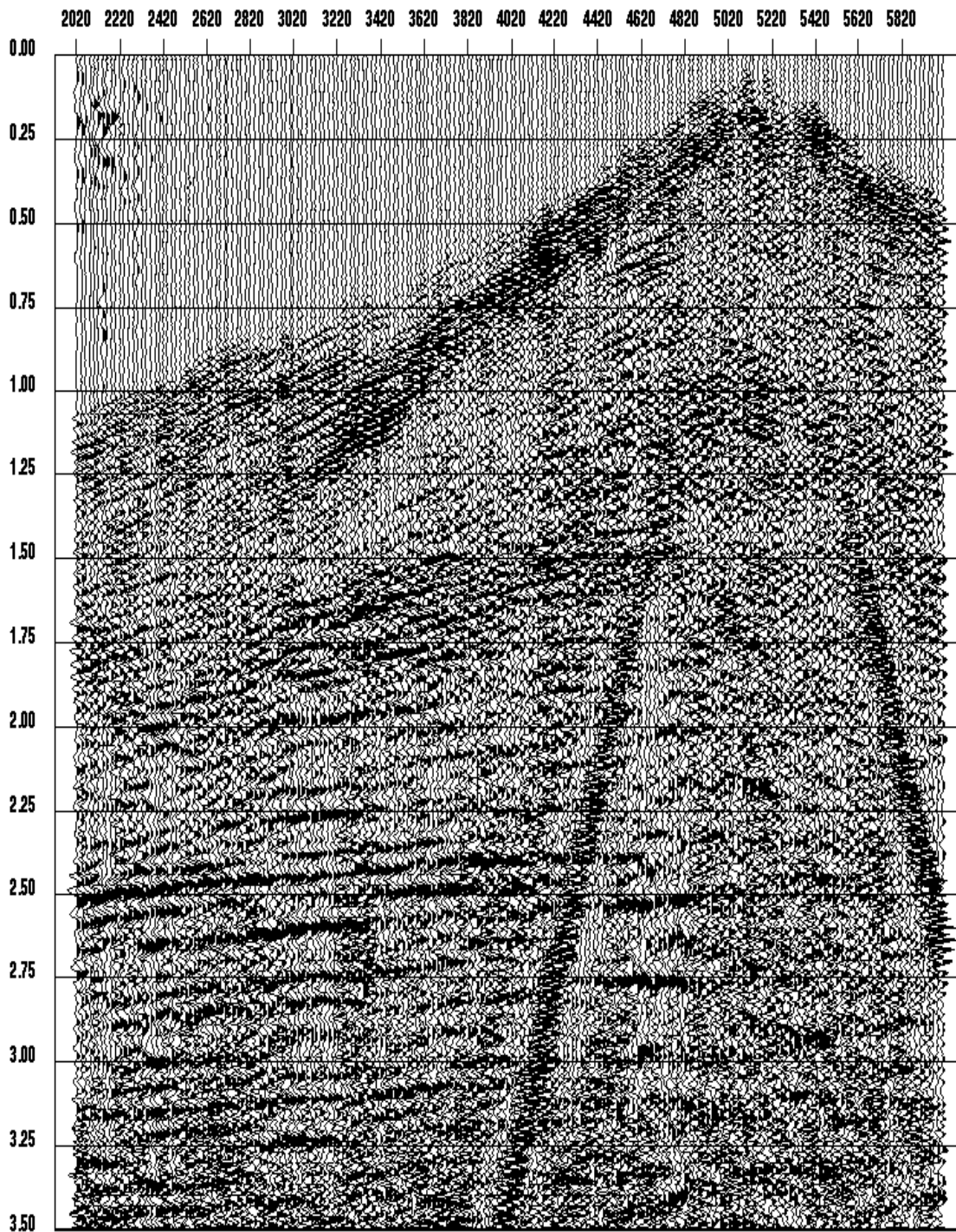


Fig. 16. Shot record at 5120 with f-x residual receiver statics applied.

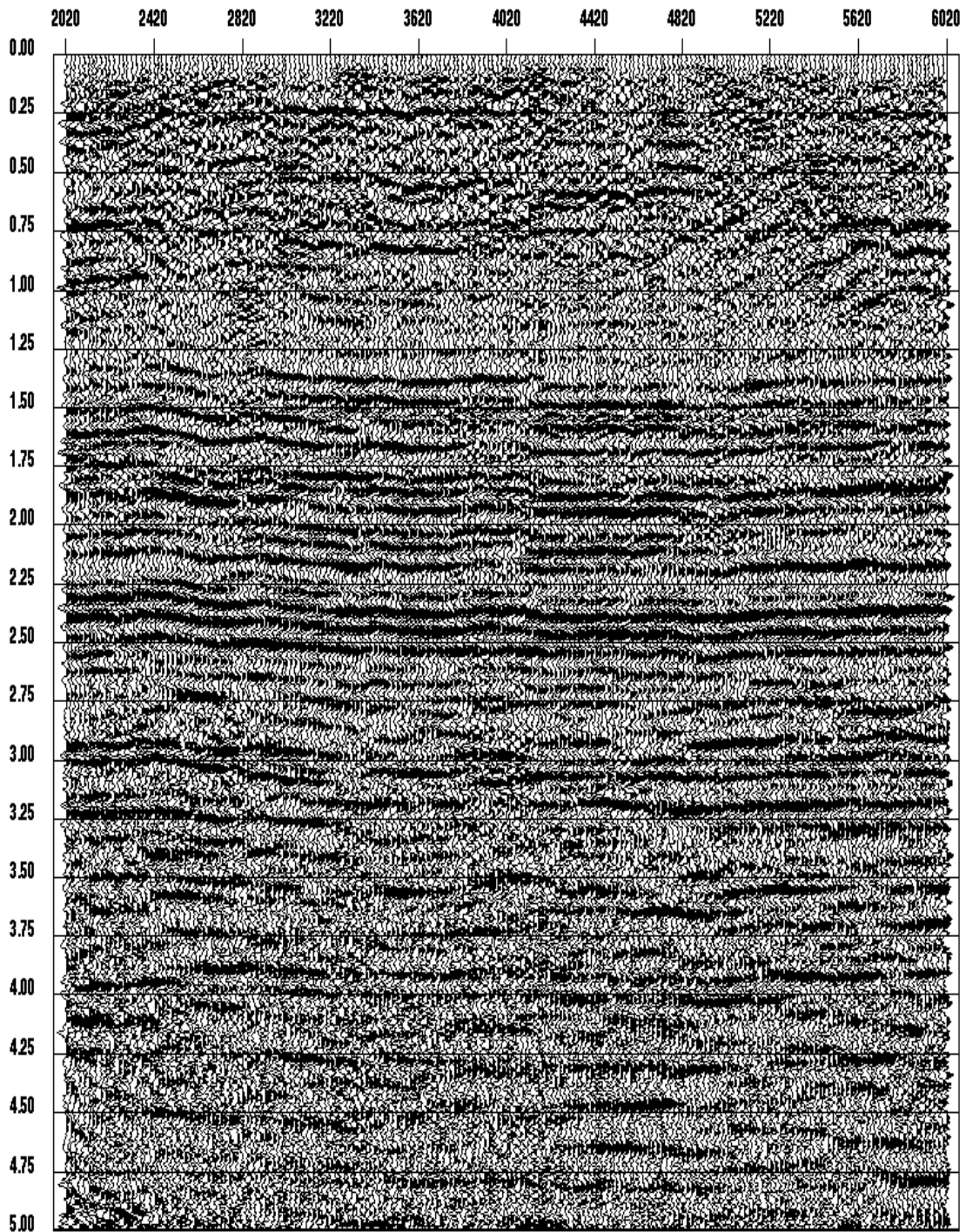


Fig. 17. Receiver stack without residual receiver statics.

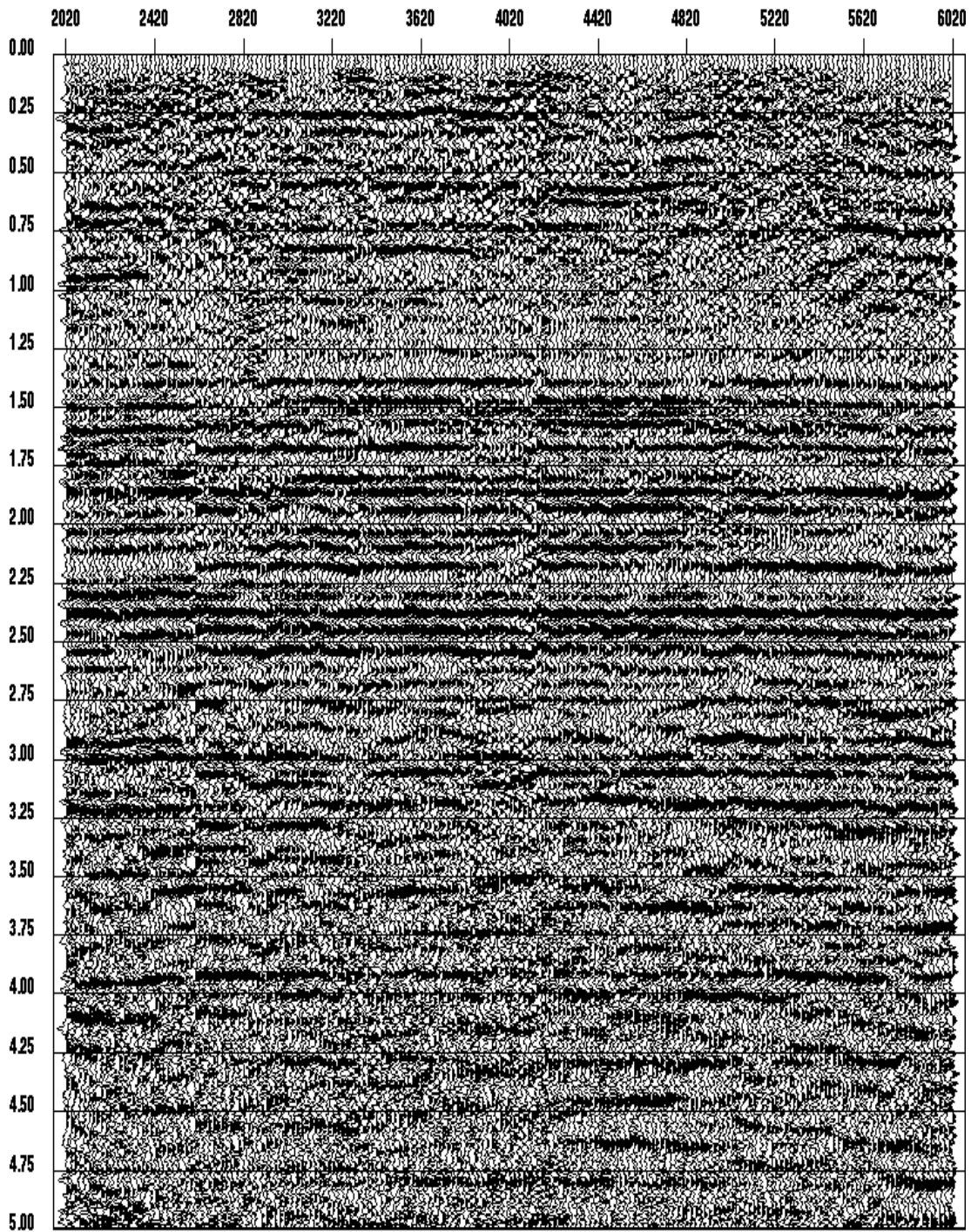


Fig. 18. Receiver stack with residual statics based on the Ronen and Claerbout algorithm. Cycle skipping is clearly seen at station 2600.

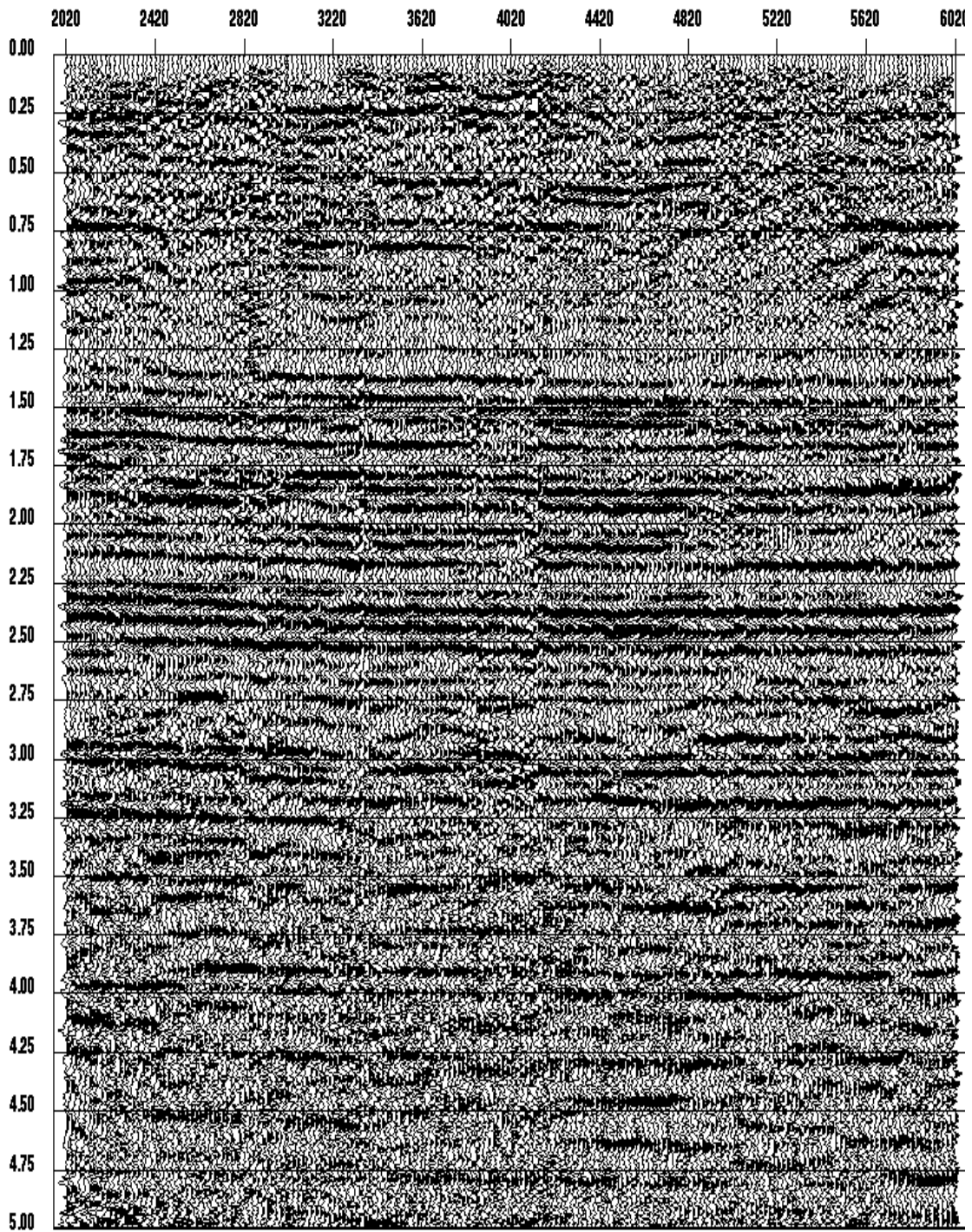


Fig. 19. Receiver stack with residual receiver statics based on f-x statics.